Green synthesis and characterization of silver nano-particles from pharmaceutically important *Periploca hydaspidis* and their biological activity

Rafi Ullah[1], Jehan Bakht[1] and Muhammad Raza Shah[2]
[1]Institute of Biotechnology and Genetic Engineering, The University of Agriculture Peshawar, KPK, Pakistan
[2]HEJ Research Institute of Chemistry, University of Karachi, Karachi, Pakistan

Abstract: The present study describes the synthesis, characterization of nano-particles from *Periploca hyaspidis* and their *in vitro* biological activity. The synthesis of AgNPs was confirmed by UV-Vis spectrophotometer and structure by atomic force microscope. The crystallite size and different functional groups was determined by X-ray diffraction and Fourier transformed infrared spectroscopy. Anti-microbial and anti-oxidant activity was carried out by disc diffusion and DPPH radical scavenging protocol respectively. Silver nano-particles (AgNPs) were synthesized by mixing 1mM $AgNO_3$ solutions with plant boiled extract in 1:9. The color change from yellow to dark brown indicated the synthesis of the nano-particles. The AgNPs were more stable at 25°C to 45°C, 1mM concentration of the salt and neutral to slightly basic pH. The results revealed that aromatic amines were responsible for the synthesis of AgNPs. The crystallite size was 7.50 nm, cubic and in nanorgime. AgNPs showed good anti-oxidant activity and was effective against *K. pnemoniae, E. coli, X. compestris, C. albicans* and *P. chrysogenum*.

Keywords: Silver nano-particles, FT-IR, XRD, AFM, *Periploca hyaspidis.*

INTRODUCTION

Plants synthesize a wide range of biologically active compounds. Being source of many powerful drugs, such medicinal plants and their derived products are known to have antibacterial, and antifungal activities etc (Bakht *et al*., 2011 a, b, c and d; 2012; 2013 a, b; 2014 a, b, c; Nasir *et al*., 2015; Amjad *et al*., 2016; Wajid *et al*., 2016; Bilal *et al*., 2017). Synthesis and characterization of nano-particles are gaining vital importance due to their wider application in different fields of physical and natural sciences (Song and Kim, 2009). In recent years, research on plants has gone through the extraordinary advancement with the production of nano-particles having controlled size and shape (Iravani, 2011). Plant mediated production of nano-particles is due to the presence of biomolecules including proteins, amino acids, vitamins, polysaccharides, polyphenols, terpeniods, and organic acids (citrates etc) present in the plants (Singh *et al*., 2016). Studies have shown that bio-molecules not only play a role in reducing the ions to the nano size, however, also play an important role in the capping of nano-particles (Collera *et al*., 2005). Over the last few decades, only prokaryotes have been exploited for their capability to bio-absorb and bio-reduce insoluble toxic metal ions to soluble non-toxic metal salts (Seshadri *et al*., 2011). However, recently it was found that highly evolved organisms like plants, algae, diatoms, human cell and other components of eukaryotes also possess the reducing potential to convert inorganic metal ions to metal nano-particles.

**Corresponding author:* e-mail: jehanbakht@yahoo.co.uk

Silver nano-particles (AgNPs) are getting immense importance because of their vital properties including high surface to volume ratios, catalytic properties and antimicrobial effects (Okafor *et al*., 2013). Majority of the techniques employed for the synthesis of nano-particles are costly and environmentally unfriendly. Silver nano-particles were synthesized extra-cellularly by the fungus *Aspergillus fumigates* (Mann, 1996). Besides microorganisms, plants can also be used for the production of nano-particles (Alia *et al*., 2015). Several plants have been successfully used for the extracellular production of silver and gold nano-particles. Leaf extracts of *Pelargonium graveolens*, *Cymbopogon flexuosus* and *Aloe vera* etc. have been used for the production of nano-particles (Shankar *et al*., 2003; Chandran *et al*., 2006). The use of plants in synthesis of nano-particles has turn out to be one of the accepted alternatives for traditional methods. The aims of the present study were the green synthesis and characterization of silver *nano-particles* from *P. hydaspidis* and to study *in vitro* biological activity of the synthesized silver nano-particles.

MATERIALS AND METHODS

Collection and identification of plant material

Plants of *Periploca hyaspidis* were collected from different parts of Swat valley (Madyan and Marghuzar) of Khyber Pukhtun Khwa (KPK) province of Pakistan. The plant was identified by plant taxonomist, Prof. Mehboob-ur-Rahman of the Department of Botany at Government Post Graduate Jahanzeb College, Swat (KPK).

Bioinspired synthesis and characterization of silver nanoparicles (AgNPs)

Preparation of plant extract

All the glass wares used for the synthesis of AgNPs were washed with aqua-regia and de-ionized water to get rid of any traces of metal contaminants. For the synthesis of AgNPs, 20g of dried grinded material of *Periploca hydaspidis* plant was soaked in 50ml of de-ionized water for 24 hours. The soaked plant material was boiled and the extract was filtered through Whatman No. 1 filter paper and used for the synthesis of nano-particles.

Biosynthesis of the nano-particles

For the synthesis of silver nano-particle, 1mM $AgNO_3$ solution was mixed with plant extract (10mg ml^{-1}) in different ratios (1:5; 1:6, 1:7, 1:8 and 1:9) with constant stirring at room temperature for 48 hours (1:1 ratio). The subsequent mixtures were prepared by increasing $AgNO_3$ until the final ratio of 1:9 was attained. The color change of the extract from yellow to dark brown indicated the formation of silver nano-particles.

UV-visible spectrophotometric study

The reduction of silver ions to AgNPs was monitored by UV-Vis spectrometry. The AgNPs solutions were diluted with deionized water in the ratio of 1:2. The UV-Vis spectral analysis was carried out using UV-Vis spectrophotometer (UV Probe, version 2.42 of Shimadzu, Japan) (Ateeq *et al*., 2015).

Atomic force microscopic analysis

Sample for AFM was prepared by dissolving a drop of NPs on the surface of mica and allowed to evaporate at ambient conditions for imaging as described by Ateeq *et al*. (2015). For the elucidation of the structure of the synthesized AgNPs, topographic images were taken using a high resolution atomic force microscope (Agilent-5500) operated in tapping mode.

X-ray diffraction (XRD) analysis

The synthesized AgNPs were freeze dried using Snidjer Freeze dryer (Snidjers Scientific Model LYSFME Holland). A few grams of freeze dried NPs were smeared uniformly onto a glass slide, assuring a flat upper surface to achieve a random distribution. The particle size and crystallite nature of the NPs were determined through X-ray diffracto-meter by step method. The X-ray diffracto-meter was equipped with target source of copper having tube voltage of 40kV, 1 degree divergence slit, 2 degree scattering slit, 0.2mm receiving slit and 2 theta ordinary mode with 2 s. The recorded data was analyzed through Origin pro 8 software. The crystallite size was calculated using Sherrer's equation.

$$Dp = 0.94\lambda/\beta_{1/2}\cos\theta$$

Where Dp is average crystallite size, λ is X-ray wavelength, β represents line broadening in radians and θ is Bragg's reflection angle (Valentina and Minaev, 2014).

Fourier transformed infrared (FT-IR) spectroscopy

FT-IR analysis was carried out by FT-IR spectrophotometer (Shimdzu IR 460). The pure plant extract and the sample containing AgNPs were freeze dried separately and analyzed through FT-IR. The various modes of vibrations were identified to determine the different functional groups present in AgNPs (Dubey *et al*., 2013).

The culture media

Nutrient agar modified media QUE-LABQB-39-3504 was used for culturing and growth of the microbes, Nutrient broth modified media QUE-LABQB-39-3504 was used for the standardization and shaking incubation of microbes (Nasir *et al*., 2015).

Microbes used for anti-microbial and fungal activities

Different bacterial and fungal strains were used as test organisms to study the anti-bacterial (Gram positive and Gram negative) and anti-fungal activities of the synthesized AgNPs (table 1 and 2). All the fungal strains were obtained from plant pathology Department, The University of Agriculture Peshawar, Pakistan.

Disc diffusion susceptibility method

The antibacterial activity of synthesized nano-particles of from *Periploca hydaspidis* was carried by disc diffusion assay as described in Bauer *et al*. (1966) against different bacterial strains. Nutrient agar media plates were inoculated with 18-24 hrs cultures of microbial inoculums (a standardized inoculums 1-2 × 107 CFU ml-1 0.5 McFarland Standard). Three discs of Whatman No. 1 filter paper (6 mm in diameter) were placed on the media in petri plates with the help of a sterile forceps. Synthesized AgNPs in different concentrations of 300, 400 and 500 ppm ml^{-1} were applied on the discs. Inoculated plates were kept at 37ºC for 18-24 hrs. The next day zones of inhibition were recorded in mm around the discs in each plate. The experiments were conducted in triplicate and the zone of inhibitions was determined by the following formula:

$$\text{Inhibition \%} - \frac{\text{Zone of sample}}{\text{Zone of control}} \times 100$$

Anti-fungal activity of the extracts through well diffusion assay

Preparation of potato dextrose agar (PDA) media for fungal cultures

Fungal strains shown in table 1 were tested for the antifungal potential of the AgNPs (Jayaseelan *et al*., 2013). The old fungal cultures were sub cultured to obtain fresh fungal cultures. Fungal strains were cultured on commercially available Potato Dextrose Agar (PDA) media. Different strains of the fungi were grown in potato dextrose agar (PDA) media and sub cultured on potato dextrose agar (PDA) media containing 104 cells ml^{-1}. Different concentrations of AgNPs (300, 400 and 500

ppm disc^{-1}) were added to the well. On the seventh day of the culturing the zone of inhibition was measured in mm. The experiments were conducted in triplicate and the zone of inhibitions was determined by the following formula.

$$\text{Inhibition \%} - \frac{\text{Zone of sample}}{\text{Zone of control}} \times 100$$

Positive control

Ciprofloxacin a broad spectrum antibiotic was used as positive control with the concentration of 50µg/6 µl for both the gram positive and gram negative bacteria while fluconazole at the same concentration was used as positive control for fungi. In both the cases DMSO was used as negative control.

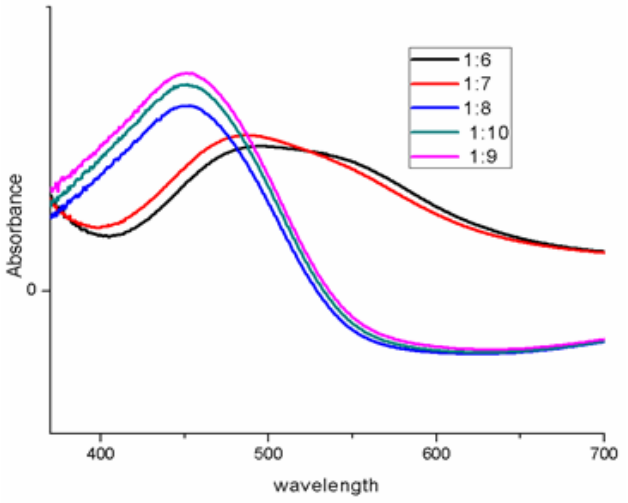

Fig. 1: Comparison of different UV-Vis spectrum of AgNPs produced by combination of *Periploca hydaspidis* plant extract (1ml) with different ratios of $AgNO_3$ (1mM) solution

DPPH radical scavenging activity

DPPH radical scavenging activity of AgNPs was determined according to the method described by Mensor *et al*. (2001). The stock solutions of the samples were diluted to final concentrations of 250, 125, 50, 25, 10 and 5µg ml^{-1} in methanol. 1ml of a 0.3mM DPPH methanol solution was added to 2.5ml solution of the extract and was allowed to react at room temperature for 30 min under complete dark. The absorbance of the resulting mixture after the reaction was taken at 518 nm using UV visible spectrophotometer. The readings were converted to percentage anti-oxidant activity (% AA) using the following formula

$Q= 100(A_o-A_s)/A_o$

Where; Q = % anti-oxidant activity, A_o =Absorbance of Pure DPPH and A_s = Absorbance of the sample.

STATISTICAL ANALYSIS

Data are shown as mean values of three replications. MSTATC computer software was used for statistical analysis (Russel and Eisensmith, 1983). Least Significant Difference (LSD) test was applied to separate differences among means Steel *et al*. (1997).

RESULTS

Bioinspired synthesis of silver nano-particles (AgNPs)

AgNPs have free electrons which give rise to Surface Plasmon Resonance (SPR). The vibration of the electrons of AgNPs collectively with the light wave produces a resonance which was detected by the detector of the UV-Vis Spectrophotometer. The synthesis of AgNPs from 1 mM solution of $AgNO_3$ was monitored and confirmed visually using UV-Vis Spectrophotometer.

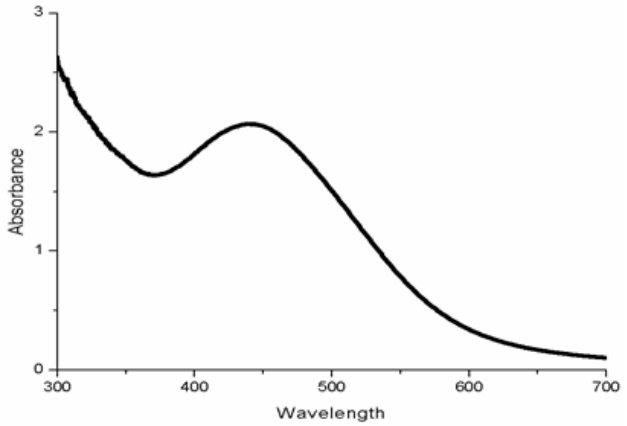

Fig. 2: UV-Vis spectrum of AgNPs produced by combination of 1 ml *Periploca hydaspidis* plant boiled extract with 9ml of $AgNO_3$ (1mM) solution. The peak of the AgNPs is at 440.41nm

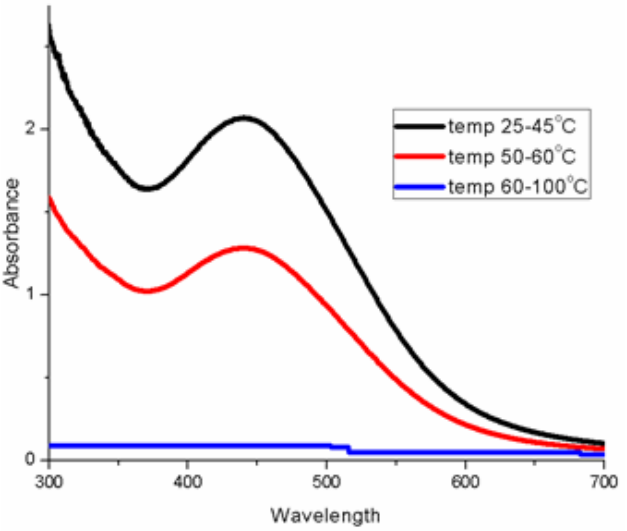

Fig. 3: UV-Vis spectrum of effect of temperature on the formation and stability of AgNPs

Visual confirmation of the synthesis

The synthesis of the AgNPs was first confirmed visually by the change in color. It was noted that the addition of

$AgNO_3$ solution to the plant extract changed the color from yellow to dark purple, which confirmed the formation of AgNPs. It was observed that gradual increase in the ratio of the plant extract to $AgNO_3$ resulted in the formation of dense color due to synthesis of large amount of nano-particles.

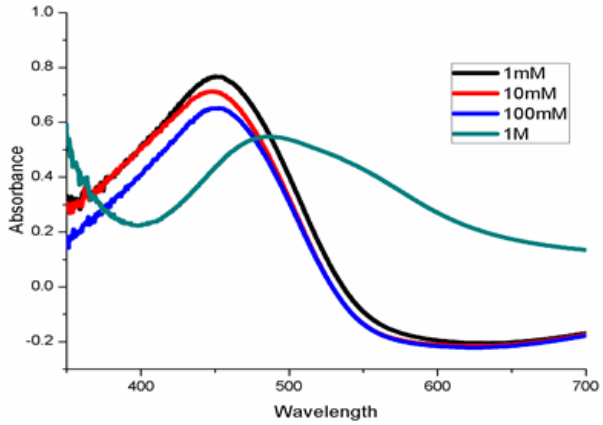

Fig. 4: Comparison of UV-Vis spectrums of AgNPs treated with different salt (NaCl) concentrations

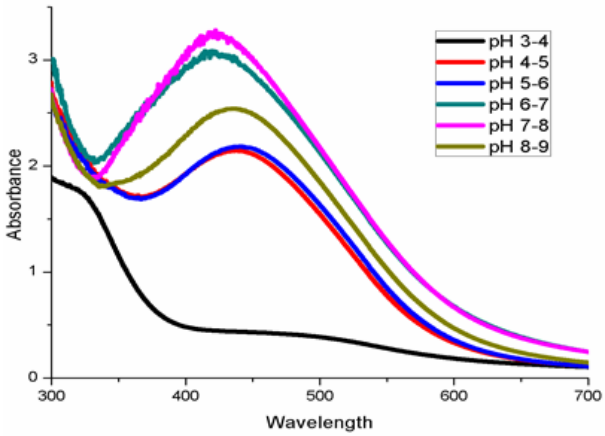

Fig. 5: Comparison of UV-Vis spectrum of AgNPs treated with different pH stress levels

UV-Vis spectrophotometeric confirmation

Fig. 1 presents UV-Vis spectrum of AgNPs formed by different ratio of the boiled plant extract with 1mM $AgNO_3$ solution. The spectrum indicated that highest peak was given by mixing of 1ml of boiled plant extract with 9 ml of $AgNO_3$ solution (1:9), while the smallest peak was observed at the ratio of 1:5. Therefore, the ratio of 1:9 (plant extract to $AgNO_3$) was used for further studies.

Confirmation of the wavelength

The synthesis of AgNPs at 1:9 ratios was further confirmed by measuring the exact wavelength at which highest absorption occurred. Fig. 2 presents the spectrum of the sample taken after 24 hours of the preparation of AgNPs. The spectrum revealed that highest absorption point (2.078) was noted at 440.41 nm, which lies in the region for absorbance of AgNPs (400 nm-500 nm).

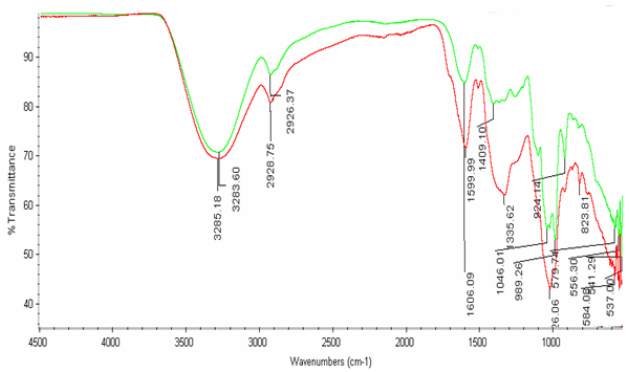

Fig. 6: Comparative FT-IR spectra of boiled plant extract and Silver Nano-particles

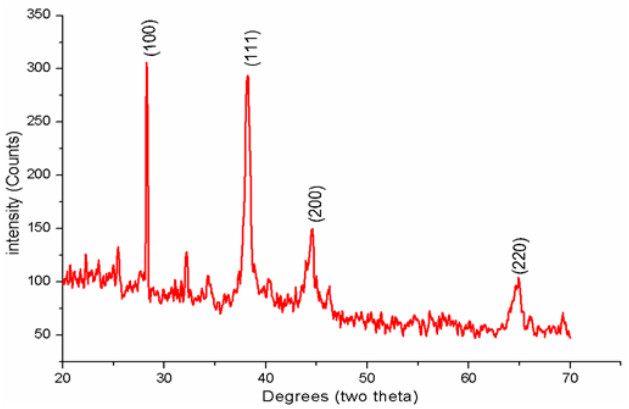

Fig. 7: XRD Patterns showing the crystallite size and nature of AgNPs

Stability study of AgNPs

Effect of temperature on AgNPs

The samples isolated at different temperatures revealed that the formation and stability of AgNPs was affected by increasing the temperature. fig. 3 demonstrated that AgNPs were most stable in the range from 25°C to 45°C measuring the highest peak. The figure also revealed that increasing temperature decreased the stability of AgNPs as indicated by the samples incubated in the range from 50°C to 60°C. The peak of the samples at this temperature was lower than measured at 24°C to 39°C which shows the deformation and destabilization of the AgNPs with elevated temperatures. The samples maintained at 60°C to 100°C indicated that most of the AgNPs were destroyed as almost no absorbance was recorded.

Effect of salt (NaCl) on AgNPs

The effect of salt stress on AgNPs stability is shown in fig. 4. The UV-Vis spectrophotogram indicated that AgNPs were more stable at mM concentrations compared with other salt levels. The figure also revealed that AgNPs were most stable at 1mM concentration and decreased with the increasing concentration of the salt. At 10mM or 100mM salt stress, the AgNPs were less stable than 1mM. The data recorded from the AgNPs treated with 1M salt revealed that the nano-particles were least stable at this

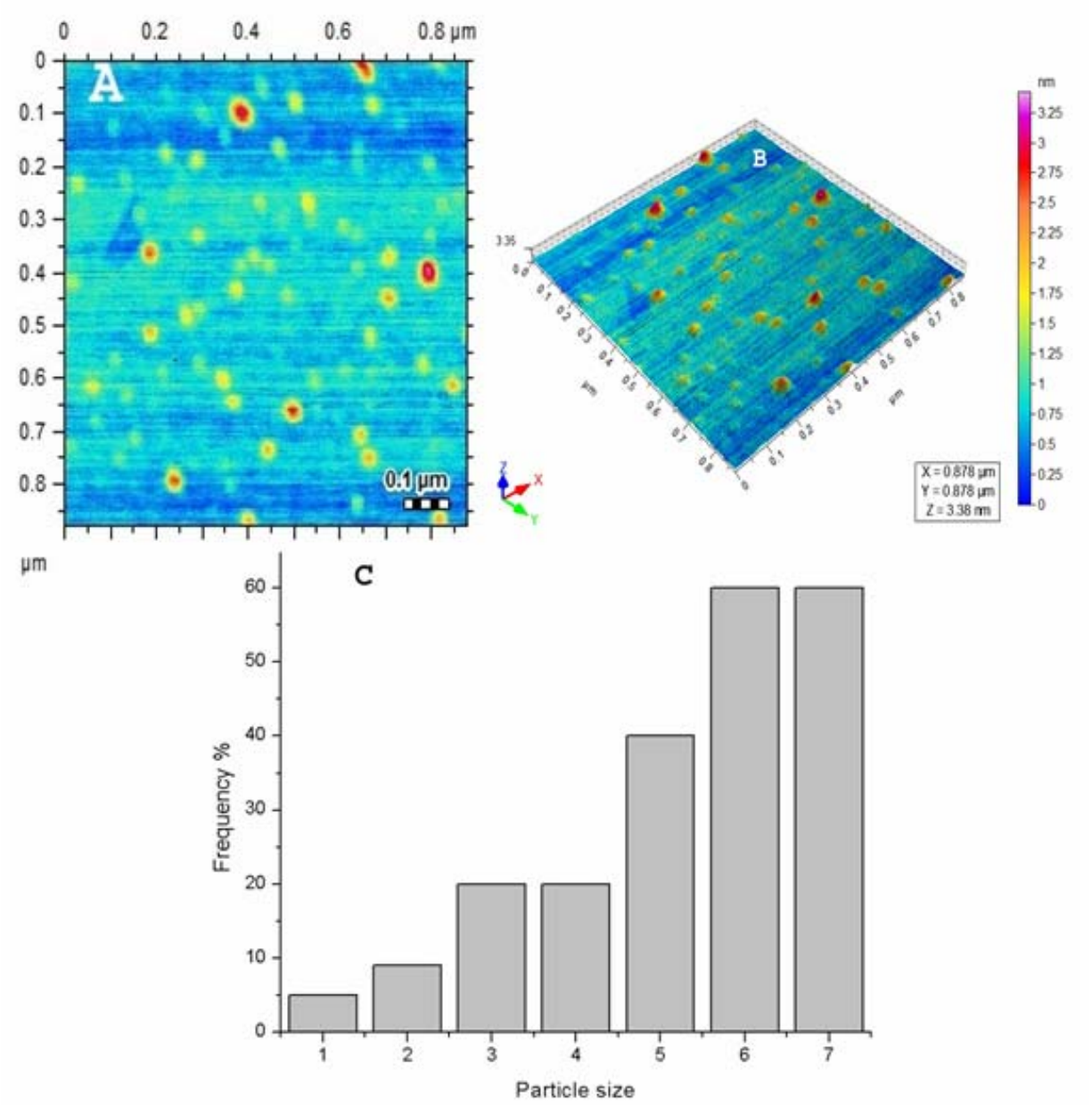

Fig. 8: AFM investigation of AgNPs (a) Topography (b) 2D view of AgNPs (c) Particle size distribution

concentration of salt as almost all the nano-particles were destroyed.

Effect of pH on AgNPs

The comparison of the peaks given by the solutions of the AgNPs subjected to different pH stress levels is given in fig. 5. The acidic pH stress was given by 1N HCl while basic pH stresses by adding 1N NaOH solutions. AgNPs formed were subjected to different pH stress levels at a broader range of pH 3 to pH 9. The AgNPs were found to be more stable at basic pH as the highest peak was measured at pH of 7-8. Generally, the AgNPs showed more stability at basic pH, as shown in the fig. 5. The AgNPs were quite stable at pH 6-7 (mildly basic) and higher pH 8-9 (basic), however, was very less stable at acidic pH of 4-5 and pH 5-6. At highly acidic pH of 3-4 almost all AgNPs were deformed and destabilized as no absorbance was measured.

FT-IR confirmation of synthesized AgNPs

The spectra of Fourier Transformed Infrared (FT-IR) Spectroscopic analysis of AgNPs are shown in fig. 6. Comparison of the FT-IR spectrum of the AgNPs and pure boiled plant extract revealed that the absorption peak at 1335.62cm^{-1} in AgNPs spectrum disappeared completely which represents aromatic amines. The disappearance of the peak suggests that the –C-N functional group containing compounds were responsible for the reduction

of Ag^{++} of $AgNO_3$ to AgNPs. A closer examination of the FT-IR spectrum of pure boiled plant extract and the synthesized AgNPs further revealed that there was a small change of ±1 to 100 wave numbers affecting the position and magnitude of the absorptions band. The shift of wave numbers from 1409.10cm^{-1} in plant extract spectra to 1335.6cm^{-1} in the spectra of AgNPs indicated that the ring aromatic compounds may also be responsible for the formation of AgNPs. A small shift of the wave numbers was also observed at the broader stretch of 3285.18 cm^{-1} to 3283.6 cm^{-1}, 2928.75 cm^{-1} to 2926.23 cm^{-1}, 1606.09 cm^{-1} to 1599.99 cm^{-1}, 1409.10 cm^{-1} to 1335.62 cm^{-1}, 1046.01 cm^{-1} to 1026.06 cm^{-1}, 924.14 cm^{-1} to 823.81 cm^{-1} between AgNPs spectra and boiled plant spectra respectively.

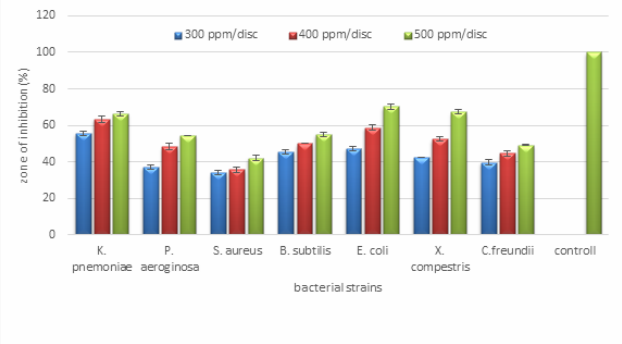

Fig. 9: Antibacterial activity of AgNPs of boiled extract of the plant against different bacterial strains by disc diffusion assay (Bar Shows LSD at P<0.05).

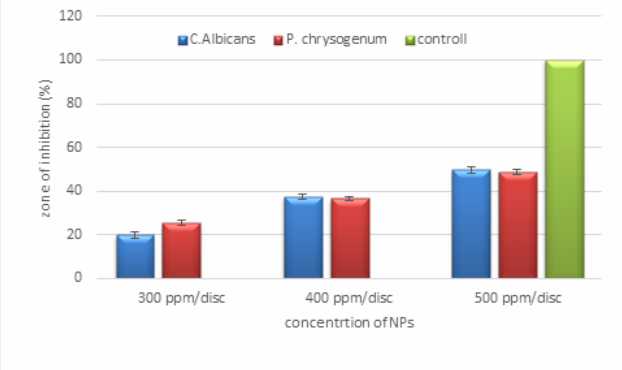

Fig. 10: Antifungal activity of AgNPs against *C. albicans* and *P. chrysogenum* (Bar Shows LSD at P<0.05)

X-Ray Diffraction (XRD) analysis of AgNPs

The XRD patterns of AgNPs synthesized from boiled plant extract is shown in fig. 7. The two theta (2θ) valves of a number of Bragg's reflections were 28.42°, 38.03°, 46.18° and 63.43° corresponding to (100), (111), (200) and (220) facets of AgNPs which may be manifested as the bands for face centered cubic structures of Ag. The XRD pattern of the freeze dried samples clearly indicated that AgNPs synthesized by the studied procedures was highly crystalline in nature. The average size of AgNPs revealed that the nano-crystallite size of AgNPs was 7.50 nm which is in agreement with AFM data. The sharpness of the first and second peaks clearly indicated that the AgNPs synthesized were in nano region. The results further revealed that there were no peaks for the XRD patterns due to the crystallographic impurities showing that the AgNPs were highly in pure form.

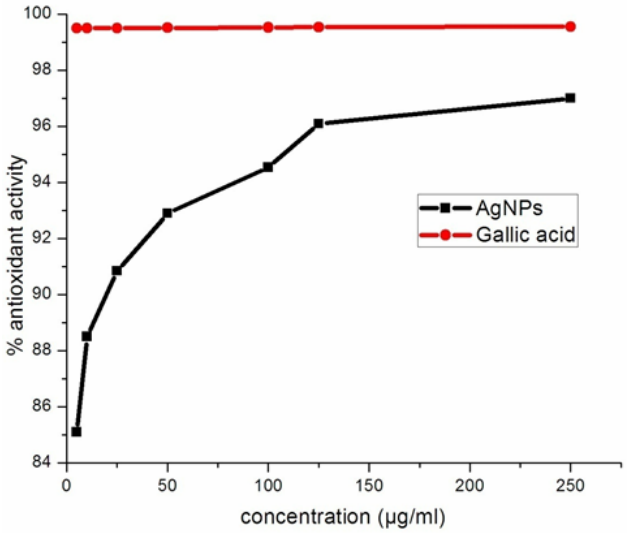

Fig. 11: Anti-oxidant activity of AgNPs measured at different concentrations.

Determination of silver nano-particles size by Atomic Force Microscope (AFM)

The particle size and its morphology were determined by AFM (fig. 8). The results revealed that the prepared particles were of different sizes. The diameter of the smallest nano-particles was found to be 1nm while the largest nano-particle was 7.5nm.The data further indicated that 60% of the synthesized particles were in the range of 6-7nm, 5% in the range of 1nm, 10% in the range of 2nm, 20% in the range of 3nm and 4nm while 40% of the AgNPs were in the range of 5nm.

Anti-microbial activity of AgNPs

The anti-bacterial activity of AgNPs is shown in Fig. 9. The data indicated that maximum zone of inhibition was measured by AgNPs at 500ppm against *X. compestris* (67.45%) and minimum zone of inhibition was demonstrated at 300ppm against *S. aureus* (33.91%). *K. pnemoniae, E. coli* and *X. compestris* were highly susceptible to AgNPs, *P. aeroginosa* and *B. subtilis* were moderately sensitive to AgNPs while *S. aureus and C. freundii* were less sensitive to AgNPs. The data suggested that the anti-bacterial activity of AgNPs was dose dependent and increasing concentration of the nano-particles also increased its activity. Fig. 10 presents the data concerning the anti-fungal activity of AgNPs of *Periploca hydaspidis* against *C. albicans* and *P. chrysogynum. C. albicans* was sensitive to AgNPs when screened at different concentrations. The data indicated that highest zone of inhibition was shown by AgNPs at 500ppm (49.69%) followed by 27.60% at 400 ppm. The

Table 1: Bacterial and fungal strains used during the present study and their origin

Microbial Species	Details
Klebsiella pneumonia (Gram Negative)	Clinical isolate, Quaid-E-Azam University Islamabad Pakistan.
Pseudomonas aeruginosa (Gram Negative)	ATCC # 9721
Staphylococcus aureus (Gram Negative)	ATCC # 6538
Bacillus subtilis (Gram Negative)	Clinical isolate, Quaid-E-Azam University Islamabad Pakistan.
Escherichia coli (Gram Negative)	ATCC # 25922
Xanthomonas campestris (Gram Negative)	ATCC # 33913
Citorbacter freundii (Gram Negative)	ATCC # 8090
Candida albicans	ATCC #10231 Plant Pathology Department The University of Agriculture Peshawar, Pakistan
Trichoderma reesei	ATCC #26921 Plant Pathology Department The University of Agriculture Peshawar, Pakistan
Acremonium alternatum	ATCC #60645 Plant Pathology Department The University of Agriculture Peshawar, Pakistan
Penicillium chrysogenum	ATCC #11709 Plant Pathology Department The University of Agriculture Peshawar, Pakistan
Rhizopus oryzae	ATCC # 20344Plant Pathology Department The University of Agriculture Peshawar, Pakistan

lowest zone of inhibition (20.00%) was measured at 300 ppm. The data exhibited that *P. chrysogynum* was susceptible to AgNPs at all concentrations used. Highest zone of inhibition was measured by AgNPs (48.99%) at 500ppm followed by 400 ppm (36.57%). The lowest zone of inhibition was measured at 300 ppm (25.46% ZI).

Anti-oxidant activity of AgNPs

The anti-oxidant activity of AgNPs was assayed through DPPH scavenging method. The data presented in fig. 11 indicated that anti-oxidant activity increased with increasing concentration of the extract. Maximum anti-oxidant activity (96%) was shown by AgNPs at 250 µg/ml concentration and minimum at 5µg/ml.

DISCUSSION

The synthesis of AgNPs from 1mM solution of $AgNO_3$ was monitored and confirmed visually and UV-Vis spectrophotometeric analysis. After addition of the $AgNO_3$ solution to the plant extract, the color of the extract changed from yellow to dark purple, which may confirmed the formation of AgNPs. The color change may be due to the reduction of the compounds present in the extract which may be responsible for the synthesis of the nano-particles (Kouvaris *et al*., 2012). The vibration of the electrons of AgNPs along with the light wave produced resonance which can be detected by UV-Vis spectrophotometer. Different ratios of 1mM solution of $AgNO_3$ and plant extract were studied for the synthesis of the AgNPs. The highest peak was given by mixing of 1ml of boiled plant extract and 9 ml of $AgNO_3$ (1:9 ratio), while the smallest peak was produced at the ratio of 1:5. Increasing amount of the $AgNO_3$ resulted in blue shift indicating the instability and destruction of the synthesized nano-particles. The instability and destruction of the nano-particles may be due the less availability of the Ag ions or the total engagement of the compounds responsible for the formation of the AgNPs (Umoren *et al*., 2014). The spectrum also revealed that the highest absorption was observed at 440.41nm, which lied in the absorbance region of the AgNPs (400nm-500nm).

The effects of different stresses like heat, pH and salt were also investigated on the stability and synthesis of AgNPs. Each stress imparted a unique effect on the stability and synthesis of AgNPs. Temperatures of the reaction play a significant role in the synthesis of nano-particles which control the nucleation process in configuration of the nano-particles (Bashir *et al*., 2013). Generally, the reaction rate increases with the increase in temperature due to amplification of molecular kinetic energy resulting on enhanced collision of the molecules. This increase in the reaction rate goes to certain limit beyond which the components of the reaction are destroyed (Vijay *et al*., 2014). The results indicated that formation and stability of AgNPs was significantly affected by increasing temperature. AgNPs were most stable at temperature range of 25°C to 45°C showing the highest peak. These results are in close agreement with Ganesan *et al*. (2013) who reported that best synthesis of AgNPs was in the range of 20°C to 50°C. The increase in temperature enhanced the absorbance of the reaction mixture resulting in greater synthesis of AgNPs. Furthermore, better SPR peaks were exhibited at this temperature with narrow absorption range indicating the stringent disparity of the synthesized AgNPs. Further increase in temperature range beyond 45°C, decreased the stability of AgNPs. The peak of the samples isolated at 50°C to 60°C was lower than at 24°C to 39°C which shows the deformation and destabilization of the AgNPs with elevated temperatures. Most of the AgNPs were destroyed at 60°C to 100°C as almost no absorbance was recorded (Bashir *et al*., 2013).

Different concentrations of the salt exerted varying effects on the formation and stability of AgNPs. AgNPs were more stable at mM concentrations compared with higher concentration. Our studies also revealed that AgNPs were most stable at 1mM concentration and stability decreased as the concentration of the salt increased. The order of stability was 1mM >10mM >100mM >1M salt. This may be due to the fact that higher concentration of sodium and chloride ions masked the synthesized AgNPs (Noruzi *et al*., 2011). The effect of pH on the stability and formation of AgNPs was also studied using UV-Vis spectrophotometer. AgNPs were subjected to different pH stress levels at a broader range of pH 3 to 9. The data indicated that pH played a significant role in the synthesis and stability of AgNPs by controlling the shape, size and cystallinity of the AgNPs (Bashir *et al*., 2013). It has been found that at lower acidic pH, large sized AgNPs were synthesized or almost no synthesis occured, while at higher alkaline/basic pH more stable and smaller size AgNPs were produced, which is in conformity with Ashok *et al*. (2010) and Amit *et al*. (2013). They concluded that AgNPs were more stable at basic pH. AgNPs were found to be more stable at mildly acidic to neutral pH as highest peak was given by the AgNPs adjusted at pH 6-7. The studies of Bashir *et al*. (2013) demonstrated that pH had a significant effect on the size, shape and hence the stability of the AgNPs and found out that the aggregation of AgNPs were likely to outclass the nucleation process at lower acidic pH, though at basic pH a great number of nuclei formation occurred, instead of aggregation, more smaller size and stable AgNPs were synthesized. In fig. 5, the blue shift demonstrated the synthesis of smaller sized AgNPs having very small diameter. Moreover, Ravichandran *et al*. (2011) reported that lower acidic pH decreased the synthesis of AgNPs while the higher basic pH increased its production. The synthesis and stability of AgNPs was adversely affected both at much higher acidic and basic pH, while stable particles were synthesized at neutral to mildly basic pH. At higher acidic and basic pH aggregation of nano-particles occurred which may be responsible for its disintegration, while at neutral to mildly basic pH no aggregation of AgNPs occurred resulting in sharp and highest peak. It was also noted that at highly acidic and basic pH no synthesis of AgNPs occurred which possibly will be due to the fact that higher positive charge at the surface of AgNPs attracted the negative charge biomass which led to flocculation (Krishnaraj *et al*., 2012).

Comparison of the FT-IR spectrum of the AgNPs and pure boiled plant extract indicated that the absorption bands at 1335.62cm^{-1} in AgNPs spectrum completely disappeared revealing aromatic amines. These results suggested that the -C-N functional group containing compounds might be responsible for the reduction of Ag^{++} to AgNPs. This may be due to the presence of the lone pair of electrons on N atom (Ravichandran *et al*., 2011). It is the first time confirmed that aromatic amines are responsible for the formation of AgNPs. FT-IR spectrum of pure boiled plant extract and the synthesized AgNPs also revealed that there was a small change of ±1 to 100 wave numbers affecting the position and magnitude of the absorptions bands. The shift of wave numbers from 1409.10 cm^{-1} in boiled plant extract to 1335.6cm^{-1} in AgNPs representing the ring aromatic compounds may also be responsible for the formation of AgNPs (Linga and Savithramma, 2012). A small shift of the wave numbers can also be seen at the broader stretch between AgNPs and boiled plant extract spectrum.

The XRD was carried out to determine the nature and size of crystallite of synthesized AgNPs from boiled plant extract of *Periploca hydaspidis.* The two theta (2θ) valves of a number of Bragg's reflections were 28.42°, 38.03°, 46.18° and 63.43° which corresponds to (100), (111), (200) and (220) facets of AgNPs which may be manifested as the bands for face centered cubic structures of Ag (Logeswari *et al*., 2013; Ganesan *et al*., 2013). The XRD pattern of the freeze dried sample of AgNPs clearly indicated that AgNPs synthesized by the current procedures were highly crystalline in nature (Ganesan *et al*., 2013). The sharpness of the first and second peaks clearly indicated that the synthesized AgNPs were in nano region. It is further revealed that there were no peaks for the XRD patterns due to the crystallographic impurities showing purity of the AgNPs. The AFM analysis revealed that the prepared particles were of different sizes. The diameter of the smallest nano-particles was found to be 1 nm while the diameter of the largest nano-particle was measured to be 7.5 nm. These results are in complete agreement with XRD data.

The anti-bacterial activity of AgNPs was also carried out during the present study. The results suggested that all the tested bacterial stains used were susceptible to all concentrations of AgNPs used and the activity of AgNPs was dose dependent. The data revealed that maximum zone of inhibition was shown by the AgNPs at highest concentration against *X. compestris* and minimum zone of inhibition was demonstrated at lowest concentrations against *S. aureus*. *K. pnemoniae, E. coli* and *X. compestris* were highly susceptible to AgNPs, *P. aeroginosa* and *B. subtilis* were moderately sensitive and *S. aureus and C. freundii* were less sensitive to AgNPs. This may be due to the fact that silver itself also possesses antimicrobial property, however, in the present study we used milli molar concentrations which outclass the said possibility. On the other hand, NPs are efficient drug carriers which may have delivered the extract efficiently. Similar results are also reported by Ameer *et al*. (2009), Me´ndez *et al*. (2011), Prasad *et al*. (2011), Sarvesh *et al*. (2013), Malarkodi *et al*. (2013), Logeswari *et al*. (2012; 2013), Nagaraj *et al*. (2014) and Kumar *et al*. (2014). The antifungal activity of AgNPs of *Periploca hydaspidis*

against *C. albicans* and *P. chrysogynum* revealed that the tested microbes were responsive to AgNPs at all concentrations used. Our data further revealed that highest zone of inhibition was established at maximum concentration of the AgNPs and lowest activity was shown at minimum levels of AgNPs. Jonny *et al*. (2014) concluded similar results against different fungal strains.

Compounds having the ability to scavenge free radicals are produced by the natural machinery of the plants. These compounds include phenolic acids, lignins, tannins, alkaloids, terpenoids, flavonoids, stilbenes, coumarins, amines and vitamins etc. (Cai *et al*., 2003). Some of these compounds have anti-inflammatory, antimutagenic, antibacterial, antiviral, antiatherosclerotic, antitumor, and anticarcinogenic activities (Sala *et al*., 2002). Ingestion of natural anti-oxidants through diet or through medicine prepared from plants can reduce the risk of happening of cancer, heart disease, diabetes, and other complications caused by the presence of free radicals (Veerapur *et al*., 2009). The quality of food products can be improved by accretion of anti-oxidants (Cook and Samman, 1996). DPPH free radical scavenging assay was carried out for the determination of anti-oxidant activity of AgNPs. It has been revealed that anti-oxidant activity was dose dependent. Highest anti-oxidant activity was noted at highest concentration of the AgNPs.

CONCLUSION

AgNPs were more stable at 25°C to 45°C, 1mM concentration of the salt and neutral to slightly basic pH. Aromatic amines were responsible for the synthesis of AgNPs. The crystallite size was 7.50 nm, cubic and in nanorgime. AgNPs showed good anti-oxidant and anti-microbial activities.

ACKNOWLEDGMENTS

The authors acknowledges the financial support of Higher Education Commission Islamabad Pakistan

REFERENCES

Alia M, Kim B, Belfield KD, Norman D, Brennan M and Ali GS (2015). Green synthesis and characterization of silver nano-particles using *Artemisia absinthium* aqueous extract-A comprehensive study. *Mater. Sci. Engg. C.,* **58**: 359-365.

Ameer A, Ahmed F, Arshi N, Chaman M and Naqvi AH (2009). One step synthesis and characterization of gold nano-particles and their antibacterial activities against *E. coli* (ATCC 25922 strain). *Int. J. Theor. Appl. Sci*., **1**: 1-4.

Amit KM, Chisti Y and Banerjee UC (2013). Synthesis of metallic nano-particles using plant extracts. *Biotechnol. Adv.,* **31**: 346-356.

Amjad U, Arshad I, Bakht J, Khalid N and Naushad A (2016). *In vitro* antimicrobial activities of different solvent extracted samples from *Iris germinica*. *Pak. J. Pharm. Sci.,* **29**: 145-150.

Ashok B, Joshi B, Kumar AR and Zinjarde S (2010). Banana peel extract mediated novel route for the synthesis of silver nano-particles, *Colloids and Surf. A: Physicochem. Engg. Aspects,* **368**: 58-63.

Ateeq M, Shah MR, Ain N, Bano S, Anis I, Faizi LS, Bertino MF and Naz SS (2015). Green synthesis and molecular recognition ability of patuletin coated gold nano-particles. *Biosen. Bioelectr.,* **63**: 499-505.

Bakht J, Tayyab M, Ali H, Islam A and Shafi M (2011a). Effect of different solvent extracted samples of on bacteria and fungi. *Afr. J. Biotechnol*., **10**: 5910-5915.

Bakht J, Ali H, Khan MA, Khan A, Saeed M, Shafi M, Islam A and Tayyab M (2011b). Anti microbial activities of different solvents extracted samples of *Linum usitatissimum* by disc diffusion. *Afr. J. Biotechnol*., **10**: 19825-19835.

Bakht J, Islam A and Shafi M (2011c). Antimicrobial potential of *Eclipta alba* by well diffusion method. *Pak. J. Bot.,* **43**: 161-166.

Bakht J, Islam A, Tayyub M, Ali H and Shafi M (2011d). Anti-microbial potentials of *Eclipta alba* by disc diffusion method. *Afr. J. Biotechnol*., **10**: 7668-7674.

Bakht J and Azra Shafi M (2012). Anti-microbial activity of *Nicotiana tobaccum* using different solvent extracts. *Pak. J. Bot*., **44**: 459-463.

Bakht J, Khan S and Shafi M (2013a). Anti-microbial potentials of fresh *Allium cepa* against gram positive and gram negative bacteria and fungi. *Pak. J. Bot*., **45**: 1-6.

Bakht J and Azra Shafi M (2013b). Anti-microbial potential of different solvent extracts of tobacco (*Nicotiana rustica*) against gram negative and positive bacteria. *Pak. J. Bot*., **45**: 643-648.

Bakht J, Shehla K and Shafi M (2014a). *In vitro* anti-microbial activity of *Allium cepa* (dry bulbs) against Gram positive and Gram-negative bacteria and fungi. *Pak. J. Pharm. Sci.,* **27**: 139-145.

Bakht J, Shaheen S and Shafi M (2014b). Antimicrobial potentials of *Mentha longifolia* by disc Diffusion method. *Pak. J. Pharm. Sci.,* **27**: 939-945.

Bakht J, Gohar N and Shafi M (2014c). *In vitro* antibacterial and antifungal activity of different solvent extracted samples of *Alhagi maurorum*. *Pak. J. Pharm. Sci.,* **27**: 1955-1961.

Bakht J, Fatema S and Shafi M (2015). Screening of *Vinca rosea* for their antibacterial and antifungal activity by disc diffusion assay. *Pak. J. Pharm. Sci.,* **28**: 833-839.

Bashir B, Ali J and Bashir S (2013). Optimization and effects of different reaction conditions for the bioinspired synthesis of silver nano-particles using *Hippophae rhamnoides* Linn. leaves aqueous extract. *World Appl. Sci. J.,* **22**: 836-843.

Bilal MK, Bakht J and Shafi M (2017). Screening of leaves extracts from *Calamus aromaticum* for their antimicrobial activity by disc diffusion assay. *Pak. J. Pharm. Sci.,* **30**: 793-800.

Cai YZ, Sun M and Corke H (2003). Anti-oxidant activity of betalains from plants of the amaranthaceae. *J. Agric. Food Chem*., **51**: 2288-2294.

Chandran SP, Chaudhary P, Pasricha R, Ahmad A, Sastry M (2006). Synthesis of gold nanotriangles and silver nano-particles using *Aloe vera* plant extract. *Biotechnol. Progr.,* **22** : 577-583.

Collera ZO, Jimenez FG, Gordillo RM (2005). Comparative study of carotenoid composition in three Mexican varieties of *Capsicum annuum* L. *Food Chem.,* **90**: 109-114.

Cook NC and Samman S (1996). Flavonoids-chemistry, metabolism, cardioprotective effect and dietary sources. *The J. Nutr. Biochem.,* **7**: 66-76.

Dubey SP, Dwivedi AD, Lahtinen M, Lee C, Kwon Y, Sillanpaa M (2013). Protocol for development of various plants leaves extract in single-pot synthesis of metal nano-particles. *Spectrochimica Acta Part A: Molecu. Biomolec. Spectro*., **103**: 134-142.

Ganesan V, Astalakshmi A, Nima P and Arunkumar C (2013). Synthesis and characterization of silver nano-particles using *Merremia tridentata* (L.) Hall. *F. Int. J. Curr. Sci*., **6**: E87-E93.

Iravani S (2011). Green synthesis of metal nano-particles using plants. *Green Chem*., **13**: 2638-2650.

Jayaseelan C, Ramkumar R, Rahuman A and Perumal P (2013). Green synthesis of gold nano-particles using seed aqueous extract of *Abelmoschus esculentus* and its antifungal activity. *Indust. Crops Prod.,* **45**: 423-429.

Jonny D, Kundu V, Kumar S, Kumar R and Chakarvarti SK (2014). Eco-friendly synthesis and characterization of silver nano-particles and evaluation of their antibacterial activity. *Am. J. Mater. Sci. Technol.,* **3**: 13-21.

Kouvaris P, Delimitis A, Zaspalis V, Papadopoulos D, Sofia A (2012). Green synthesis and characterization of silver nano-particles produced using *Arbutus unedo* leaf extract. *Mater. Lett.,* **76**: 18-20.

Krishnaraj C, Ramachandran R, Mohan K and Kalaichelvan PT (2012). Optimization for rapid synthesis of silver nano-particles and its effect on phytopathogenic fungi. *Spectrochim. Acta. Part A: Molec. Biomolec. Spectro.,* **93**: 95-99.

Kumar GV, Gokavarapub SD, Rajeswarib A, Dhasa TS, Karthicka V, Kapadiab Z, Shresthab T, Barathyb IA, Royb A and Sinhab S (2011). Facile green synthesis of gold nano-particles using leaf extract of antidiabetic potent *Cassia auriculata. Colloids and Surf. B: Biointer.,* **87**: 159-163.

Linga RM and Savithramma N (2012). Antimicrobial activity of silver nano-particles synthesized by using stem extract of *Svensonia hyderobadensis* (Walp.) Mold- A rare medicinal plant. *Res. Biotechnol*., **3**: 41-47.

Logeswari P, Silambarasan S and Abraham J (2013). Eco-friendly synthesis of silver nano-particles from commercially available plant powders and their antibacterial properties. *Scientia Iranica,* **3**: 1049-1054.

Logeswari P, Silambarasan S and Abraham J (2012). Synthesis of silver nano-particles using plants extract and analysis of their antimicrobial property. *J. Saudi Chem. Soc*., **48**: 1-7.

Malarkodi C, Rajeshkumar S, Vanaja M, Paulkumar K, Gnanajobitha G, Annadurai G (2013). Eco-friendly synthesis and characterization of gold nano-particles using *Klebsiella pneumoniae*. *J. Nanostruct. Chem*., **3**: 30-37.

Mann S (1986). Biomimetic Materials Chemistry. VCH, New York.

Me´ndez MAA, Martı´n-Martı´nez ES, Ortega-Arroyo L, Portillo GC and SEspı´ndol E (2011). Synthesis and characterization of silver nano-particles: effect on phytopathogen *Colletotrichum gloesporioides. J. Nanopart. Res*., **13**: 2525-2532.

Nagaraj B, Idhayadhulla A and Lee YR (2014). Industrial crops and products phyto-synthesis of gold nano-particles using fruit extract of *Hovenia dulcis* and their biological activities. *Indust. Crops Prod*., **52**: 745-751.

Nasir A, Dawood A and Bakht J (2015). Antibacterial activity of different solvent extracted samples from the flowers of medicinally important *Plumeria obstusa. Pak. J. Pharm. Sci*., **28**: 195-2000.

Noruzi M, Zare D, Khoshnevisan K and Davoodi D (2011). Rapid green synthesis of gold nano-particles using *Rosa hybrida* petal extract at room temperature. *Spectrochim. Acta Part A: Molec. Biomolec. Spectro.,* **79**: 1461-1465.

Okafor F, Janen A, Kukhtareva T, Edwards V and Curley M (2013). Green synthesis of silver nano-particles, their characterization, application and antibacterial activity. *Int. J. Environ. Res. Public Health,* **10**: 5221-5238.

Prasad TNVKV, Elumalai EK and Khateeja S (2011). Evaluation of the antimicrobial efficacy of phytogenic silver nano-particles. *Asian Pacif J. Trop. Biomed*., **1**: 82-85.

Ravichandran V, Tiah ZX, Subashini G, Terence FWX, Eddy FCY, Nelson J and Sokkalingam AD (2011). Biosynthesis of silver nano-particles using mangos teen leaf extract and evaluation of their antimicrobial activities. *J. Saudi Chem. Soc.,* **15**: 113-120.

Russel DF, Eisensmith SP and MSTAT-C (1983). Crop Soil Science Department, Michigan State University USA.

Sala A, Recio MD, Giner RM, Manez S, Tournier H, Schinella G and Rios JL (2002). Anti-inflammatory and anti-oxidant properties of *Helichrysum italicum*. *J. Pharma. Pharmacol.*, **54**: 365-371.

Sarvesh KS, Yamada R, Ogino C and Kondo A (2013). Biogenic synthesis and characterization of gold nano-particles by *Escherichia coli* K12 and its heterogeneous catalysis in degradation of 4-nitrophenol. *Nanoscale Res. Lett.,* **8**: 70-79.

Seshadri S, Saranya K and Kowshik M (2011). Green synthesis of lead sulfide nano-particles by the lead resistant marine yeast, *Rhodosporidium diobovatum*. *Biotechnol. Prog*., **27**:1464-1469.

Shankar SS, Ahmad A, Pasrichaa R and Sastry M (2003). Bioreduction of chloroaurate ions by geranium leaves and its endophytic fungus yields gold nano-particles of different shapes. *J. Mater. Chem.,* **13**: 1822-1826.

Singh P, Kim YJ, Zhang D and Yang DC (2016). Biological synthesis of nano-particles from plants and micro-organisms. *Trends in Biotechnol*., **34**: 588-599.

Song JY, Kim BS (2009). Rapid biological synthesis of silver nano-particles using plant leaf extracts. *Bioproc. Biosyst. Engg.*, **32**: 79-84.

Steel RGD, Torrie JH and Dickey DA (1997). Principles and procedures of statistics. *A Biometrical Approach*, 3rd Ed. McGraw Hill Book Co. Inc. New York USA. pp.172-177.

Umoren SA, Obot IB and Gasem ZM (2014). Green synthesis and characterization of silver nano-particles using red apple (*Malus domestica*) fruit extract at room temperature. *J. Mater. Environ. Sci*., **5**: 907-914.

Valentina AL and Minaev BF (2014). The size-controllable, one-step synthesis and characterization of gold nano-particles protected by synthetic humic substances. *Mater. Chem. Phys.,* **30**: 1-11.

Veerapur VP, Prabhakar KR and Parihar VP (2009). *Ficus racemosa* stem bark extract: A potent anti-oxidant and a probable natural radio protector. *Evid. Based Complem. Alterna. Med.,* **6**: 317-324.

Vijay KPPN, Pammib SVN, Kolluc P, Satyanarayanad KVV and Shameema U (2014). Green synthesis and characterization of silver nano-particles using *Boerhaavia diffusa* plant extract and their anti bacterial activity. *Indust. Crops Prod.,* **52**: 562-566.

Wajid K, Bakht J and Shafi M (2016). Antimicrobial potential of different solvent extracted samples from *Physalis ixocarpa*. *Pak. J. Pharm. Sci.,* **29**: 467-475.